The role of Ca^{2+}-activated K^+ channel spliced variants in the tonotopic organization of the turtle cochlea

E. M. C. Jones, M. Gray-Keller and R. Fettiplace

Department of Physiology, University of Wisconsin Medical School, Madison, WI 53706, USA

(Received 2 March 1999; accepted after revision 26 April 1999)

1. Turtle auditory hair cells contain multiple isoforms of the pore-forming α-subunit of the large-conductance Ca^{2+}-activated K^+ (K_{Ca}) channel due to alternative splicing at two sites. Six splice variants were studied by expression in *Xenopus* oocytes.

2. The isoforms possessed differences in apparent Ca^{2+} sensitivity and kinetics. The lowest Ca^{2+} sensitivity was observed in a novel variant resulting from a 26 amino acid deletion around one of the splice sites.

3. Co-expression of a bovine β-subunit slowed the current relaxation 10-fold compared with channels formed from α-subunits alone but preserved the original order of kinetic differences. The β-subunit also increased the Ca^{2+} sensitivity of isoforms to bring them nearer the range of sensitivity of the native K_{Ca} channels of the hair cell.

4. With channels formed from α-subunits or $\alpha + \beta$-subunits, the half-activation voltage in a fixed Ca^{2+} concentration, and the time constant of the current relaxation, varied linearly with the combined size of the insertions/deletions at the splice sites.

5. Experiments in which the β/α concentration ratio was varied indicated that the β-subunit exerts an all-or-none effect on the Ca^{2+} sensitivity and kinetics of the channel.

6. Co-expression of an avian β2-subunit had effects on kinetics and Ca^{2+} sensitivity of several α-isoforms which were qualitatively similar to those produced by the bovine β-subunit.

7. We conclude that differential expression of alternatively spliced α-subunit variants and a non-uniform distribution of a β-subunit can produce a range of K_{Ca} channel properties needed to explain the tonotopic organization of the turtle cochlea.

The large-conductance Ca^{2+}-activated K^+ (K_{Ca}) channel, often referred to as the BK channel, is a multimeric complex of a pore-forming α-subunit and a regulatory β-subunit (Kaczorowski *et al.* 1996). The α-subunit in vertebrates arises from a single *slo* gene, the alternative splicing of which produces isoforms with a range of channel properties (Butler *et al.* 1993; Tseng-Crank *et al.* 1994). Most of the known splice sites lie in the extended C-terminus that incorporates the intracellular Ca^{2+}-binding domain (Wei *et al.* 1994). The β-subunit interacts with the N-terminus of the α-subunit (Wallner *et al.* 1996) to augment the Ca^{2+} sensitivity of the channel (McManus *et al.* 1995).

An important function of neuronal K_{Ca} channels is to determine the duration of the action potential and thereby influence release of neurotransmitter (Robitaille & Charlton, 1992); however, the significance to this function of the numerous channel isoforms is obscure. K_{Ca} channels also play a special role in the electrical tuning of auditory hair cells where, in combination with voltage-dependent Ca^{2+} channels, they cause the cells to be maximally responsive to particular sound frequencies (reviewed in Wu *et al.* 1995). In the turtle cochlea, hair cells are tuned to a 20-fold range of frequencies that is determined largely by differences in the K_{Ca} channel kinetics (Art & Fettiplace, 1987; Art *et al.* 1995). Since the hair cells are arranged tonotopically (Crawford & Fettiplace, 1980), the K_{Ca} channel properties must change systematically from the apical to basal end of the organ. The mechanisms of the kinetic variation and the concomitant tonotopic organization are unknown. One possibility is the expression of channel isoforms with distinct kinetics in different regions of the cochlea (Wu & Fettiplace, 1996).

K_{Ca} channel α-subunits have recently been cloned from hair cells of both turtle (Jones *et al.* 1998) and chicken (Jiang *et al.* 1997; Navaratnam *et al.* 1997; Rosenblatt *et al.* 1997) and shown to exhibit extensive alternative splicing. Here we describe the functional consequences of these alternative splicing patterns and show that, by appropriate mixing of α-subunit isoforms with or without β-subunit, it is possible to achieve a range of properties approximating those in native hair cells.

METHODS

Turtles (*Trachemys scripta elegans*) were decapitated and the basilar papilla was isolated using procedures approved by the Animal Care Committee at the University of Wisconsin. Hair cells were enzymatically dissociated from the basilar papilla (Art & Fettiplace, 1987) and alternatively spliced Ca^{2+}-activated K^+ channel transcripts were obtained by reverse-transcriptase, polymerase chain reaction (RT-PCR) amplification of hair cell RNA as described by Jones *et al.* (1998). For studying the distribution of different transcripts, the basilar papilla was divided into four regions of equal length using a tungsten needle and cells from each region were collected separately. Splice site numbering was identical to that in Tseng-Crank *et al.* (1994) and Jones *et al.* (1998). A full-length expression construct, pGH19-X0:0, was obtained by ligating overlapping PCR fragments that encode the C-terminal two-thirds of *tSlo* (nucleotides 1085–3560) with the N-terminal of *cSlo1* (nucleotides 1–1231) into the oocyte expression vector pGH19 (Robertson *et al.* 1996). The *cSlo1* N-terminal was a gift from P. Fuchs (Johns Hopkins University, Baltimore, MD, USA) and differs from the same region in *tSlo* in seven conservative substitutions. Five of these substitutions are in the S0–S1 intracellular loop, one is in the S2 transmembrane segment and one (P/Q) is just prior to the pore. The results of Wei *et al.* (1994) demonstrate that the N-terminal region of the protein influences single-channel conductance but not other channel properties including Ca^{2+} sensitivity. Full-length expression constructs were derived by ligating *Acc*I-digested fragments from clones containing the naturally occurring combinations of alternatively spliced exons with *Acc*I-digested pGH19-X0:0. A novel *tSlo* variant was obtained by RT-PCR amplification of hair cell RNA using a forward primer specific for splice site 1 (SS1) containing SRKR, 5′ACGGGAAAGCAGAAGCCGAAA3′, and a reverse primer, 5′CTCATGCCTCCATTTCGCTGC3′, identical to a sequence downstream of splice site 2 (SS2). A full-length construct of this variant was obtained by ligating a *Bsr*DI fragment with a *Bsr*DI partial digest of pGH19-X0:0. Expression constructs were named according to the number of amino acids inserted or deleted at splice sites 1 and 2. Both strands of the X0:0 expression construct, and the 600 base pair region containing SS1 and SS2, as well as restriction sites used for subcloning all subsequent isoform expression constructs, were sequenced on an ABI automated sequencer. Bovine Ca^{2+}-activated K^+ channel β-subunit was a gift from R. Swanson (Merck Research Labs, Rahway, USA); β-subunits from quail and chicken were kindly provided by Corinna Oberst and Klaus Bister (University of Innsbruck, Austria). The cDNA for each β-subunit was ligated into the pGH19 vector for RNA production.

Capped cRNA coding for Slo variants was synthesized *in vitro* from *Xho*I-linearized expression constructs using the mMessage mMachine T7 kit (Ambion, Austin, TX, USA). *Xenopus laevis* frogs were anaesthetized with 3-amino benzoic acid ethyl ester (MS-222; 1 g l^{-1} in distilled water) and stages V and VI oocytes were isolated from their ovaries and maintained using standard procedures (Stühmer & Parekh, 1995). Within 24 h of isolation, the oocytes were injected with 10–30 ng of *Slo* variant cRNA with or without various amounts of β-subunit cRNA. Electrical recordings were made at room temperature (21–23 °C) from inside-out membrane patches excised from oocytes 4–24 days post-injection, using previously described procedures (Stühmer & Parekh, 1995). Electrodes were filled with a solution of composition (mM): 110 potassium methyl sulphate, 2 KCl, 5 K_2EGTA, 10 KHepes, pH 7·4. They had a resistance of 0·5–1 MΩ for macropatches containing 100 to 1000 channels, and 15–30 MΩ for measuring single-channel currents. Methyl sulphate was employed as the major anion to minimize interference from a Ca^{2+}-activated Cl^- current endogenous to oocytes (Stühmer & Parekh, 1995). The intracellular face of the patch was exposed to solution of composition (mM): 110 potassium methyl sulphate, 2 KCl, 2 K_4dibromoBAPTA (Molecular Probes, Eugene, OR, USA), 1 dithiothreitol, 10 KHepes, pH 7·4, with different amounts of $CaCl_2$ added to yield free Ca^{2+} concentrations from 0·3 to 20 μM. Expected free Ca^{2+} concentrations were calculated from the MaxChelator computer program (Bers *et al.* 1994). Solutions with more than 20 μM free Ca^{2+} contained no dibromoBAPTA. All Ca^{2+} activities were verified with an MI-600 Ca^{2+} electrode (Microelectrodes Inc., Londonderry, NH, USA) calibrated in a series of standard Ca^{2+} buffer solutions (Tsien & Rink, 1980). Dithiothreitol was included in the intracellular medium to prevent channel 'run-down', manifested as a loss of Ca^{2+} sensitivity during the course of a recording (Dichiara & Reinhart, 1997). Current responses were filtered with an eight-pole Bessel filter at 2·5 or 5 kHz prior to digitization and analysis. Unless otherwise stated, results are expressed as the mean ± 1 standard error of the mean (S.E.M.).

Mean open times were measured from single-channel recordings containing more than 3000 events. The records were filtered at 5 kHz (−3 dB) and digitized at 40 kHz. Open time histograms were truncated at 0·1 ms due to the 'dead time' introduced by the filter, and were fitted with the sum of two exponential components using a maximum likelihood algorithm (Art *et al.* 1995). We observed slow fluctuations in open probability similar to those reported by Silberberg *et al.* (1996) for K_{Ca} channels expressed in *Xenopus* oocytes, but there were no large concomitant variations in mean open time. For example, the open probability of a 4:−26 $\alpha+\beta$-channel cycled with a periodicity of about 50 s from 0·14 to 0·56, but the open time varied by no more than ∼15% around its mean value of 4·7 ms. Burst analysis of channel records (Colquhoun & Sackmann, 1985) was performed by considering only those events defined by closures (t_c) greater than a minimum of 0·5 ms. The value of t_c was chosen to eliminate the briefest component of the closed time distributions associated with channel 'flicker'. The burst analysis was implemented using a computer program, Channel2, written by Michael Smith of the Australian National University, Canberra, Australia.

RESULTS

Splice variants of the hair cell K_{Ca} channel α-subunit

We have identified eight alternatively spliced cDNAs homologous to the *slo* gene that encodes the K_{Ca} channel α-subunit. The proteins produced from these transcripts differed in the length of the amino acid chain linking the eighth and ninth amphipathic α-helical segments in the extended intracellular C-terminus (Fig. 1). Chain length was varied by insertion of exons at two splice sites that were labelled SS1 and SS2 according to the terminology of Tseng-Crank *et al.* (1994) who first identified these splice sites in human brain cDNA. We were unable to detect splicing at other potential sites including those recently reported nearer the 5′ end of *cSlo* from chicken basilar papilla (Navaratnam *et al.* 1997; Rosenblatt *et al.* 1997). We infer therefore that the eight variants correspond to naturally occurring combinations in turtle hair cells.

Seven of the variants, denoted by the number of amino acids inserted at SS1 and SS2, respectively, were 0:0, 4:0,

4:3, 4:61, 31:3, 31:0 and 0:3 (Jones *et al.* 1998). The 31 amino acid insert is novel and was composed of 4 + 27 amino acids, where the 4 amino acid sequence (SRKR) occurs alone in three of the other variants. The eighth variant, which is also novel, was identified by amplification of hair cell RNA using a forward primer specific for SRKR in SS1, and a reverse primer downstream of SS2. This variant was smaller than the expected 'minimal' sequence due to a 26 amino acid deletion (from residues 616 to 641 in thc1; see Jones *et al.* 1998) encompassing SS2, and has therefore been labelled 4:−26 (GenBank accession number AF086646). This variant indicates the presence of an additional splice site, SS2′, situated 36 amino acids downstream of SS1, an arrangement implying an unexpected complexity of splicing. The donor site of SS2′ lay within the codon corresponding to residue 615 of thc1, and the acceptor site of SS2′ was located within the codon of residue 641 of thc1 (see Fig. 1*C*). In two preparations, expression of the 4:−26 variant was found to

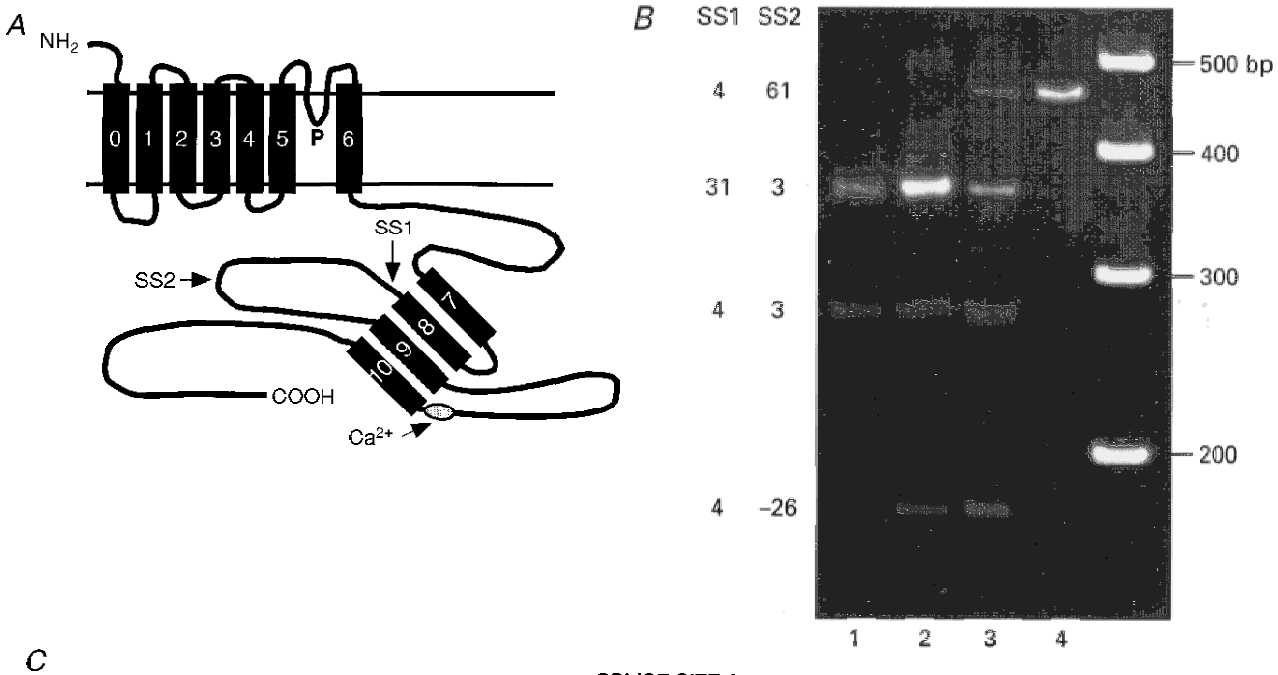

C

SPLICE SITE 1

```
0,0   (thc1)...AKLKLLMTAIEYKSEKRESS----------ILINPGNHVKTQEGTLGFFIASDAKEVKRAYFYC
4,3   (thc3)...AKLKLLMTAIEYKSEKRESRSRKR----------ILINPGNHVKIQEGTLGFFIASDAKEVKRAYFYC
4,61  (thc4)...AKLKLLMTAIEYKSEKRESRSRKR----------ILINPGNHVKIQEGTLGFFIASDAKEVKRAYFYC
31,3  (thc5)...AKLKLLMTAIEYKSEKRESRSRKRHRAQKKEAMPMSYKRCAAGIHTDPTRCILINPGNIVKIQEGTLGFFIASDAKEVKRAYFYC
4,-26 (thc7)...AKLKLLMTAIEYKSEKRESRSRKR----------ILINPGNHVKIQEGTLGFFIASDAKEVKRAYFYC
```

SPLICE SITE 2

```
      *                                                                    *
0,0   KACHDDTTDPKRIKKCGCKRL----------EDEHPSTLSP...
4,3   KACHDDITDPKRIKKCGCKRLIYF---------EDEHPSTLSP...
4,61  KACHDDITDPKRIKKCGCKRLIYSKMSIYKRMKLACCFDCGRSERDCSCMSGSVHSNMDTLERAFPLSSVSVNDCSTSLRAFEDEHPSTLSP...
31,3  KACHDDITDPKRIKKCGCKRLIYF----------EDEHPSTLSP...
4,-26 KA----------LSP...
```

Figure 1. Structure of hair cell K_{Ca} channel splice variants

A, schematic diagram of the K_{Ca} channel α-subunit, showing seven transmembrane domains, a pore (P) region, and an extended intracellular C-terminus (Meera *et al.* 1997). Positions of a putative Ca^{2+}-binding site (Schreiber & Salkoff, 1997) and the two splice sites, SS1 and SS2, are indicated. The amphipathic helical domains S7 to S10 are drawn arbitrarily in antiparallel configuration. *B*, polyacrylamide gel of PCR products from hair cells isolated from four quarters of the basilar papilla, lane 1 corresponding to apical low-frequency cells and lane 4 to basal high-frequency cells. Turtle mRNA was amplified with a forward primer specific for SS1 = 4 (SRKR), and a reverse primer downstream of SS2 (see Methods). This revealed four of the splice variants including the 4:−26 that contains a 26 amino acid deletion around SS2. The right-hand lane contains 100 bp size markers. The 31 amino acid insert in the 31:3 variant is composed of 4 amino acids (SRKR) + 27 amino acids. Note that each variant shows a different distribution. *C*, amino acid sequences in the region around SS1 and SS2 of five of the isoforms studied, with the inserts denoted in bold. The asterisks mark the donor and acceptor positions for a new splice site (see text). A sixth variant, 0:3, contained IYF in SS2. thc1, 3, 4, 5, 7 refer to the naming of the turtle hair cell Slo variants in the GenBank database.

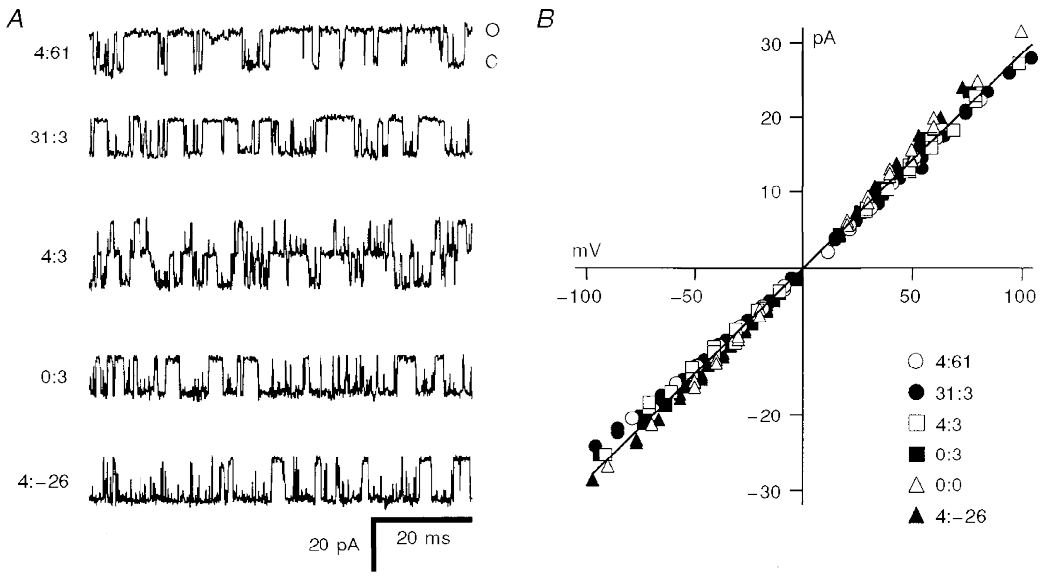

Figure 2. Examples of single K_{Ca} channels produced by expression of splice variants in *Xenopus* oocytes

A, 80 ms stretches of recordings for five of the isoforms, all measured in 50 μM Ca^{2+} at −50 mV holding potential. The isoforms, denoted by the amino acid inserts at SS1 and SS2, are given beside each trace. Current levels corresponding to the closed (C) and open (O) configuration are shown on the top trace and are the same for all variants. *B*, single-channel current–voltage relationships for channels obtained with different isoforms. Note that all have the same unitary conductance, the least-squares fit through the points corresponding to a conductance of 286 pS.

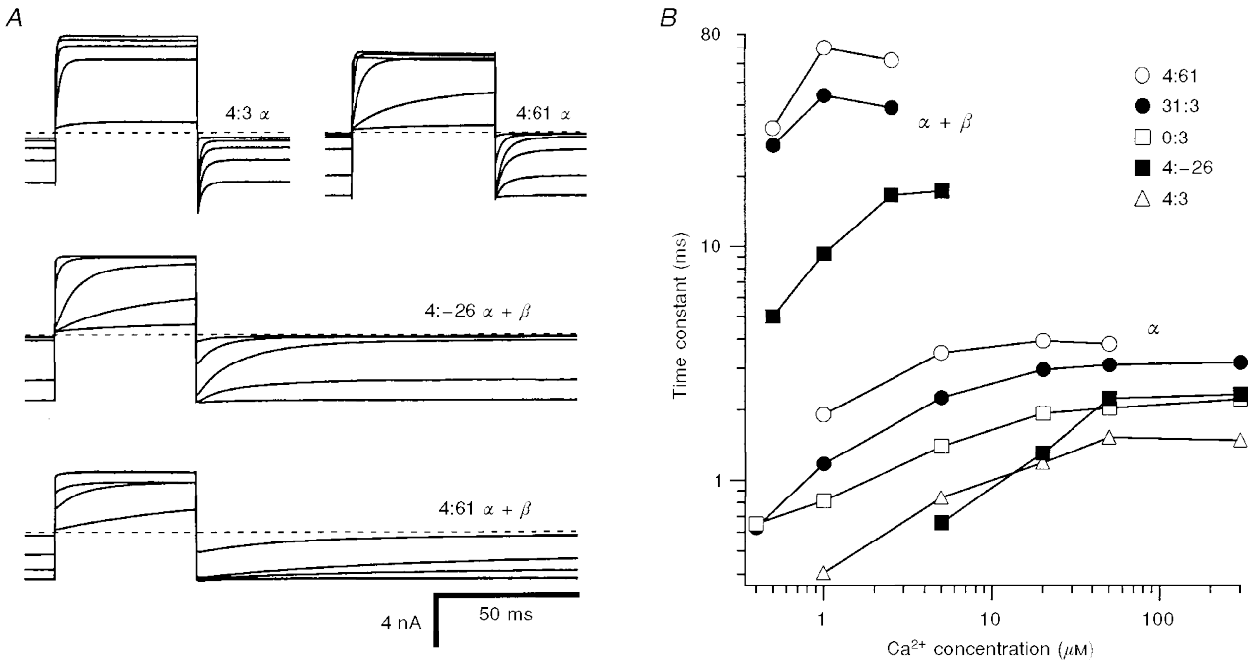

Figure 3. Properties of currents produced by expression of splice variants in *Xenopus* oocytes

A, averaged macroscopic currents for voltage steps from −50 to +50 mV in a range of intracellular Ca^{2+} concentrations. Subunit components and Ca^{2+} concentrations: 4:3 α-subunit: 1, 5, 20, 50 and 300 μM Ca^{2+}; 4:61 α-subunit: 0·4, 1, 2·5, 5, 20 and 300 μM Ca^{2+}; 4:−26 α- + bovine β-subunit: 0·4, 1·5, 2·5, 5 and 20 μM Ca^{2+}; 4:61 α- + bovine β-subunit: 0·4, 1·5, 2·5, 5 and 20 μM Ca^{2+}. Note that for offset kinetics at −50 mV, 4:3 α is faster than 4:61 α, and 4:−26 α + β is faster than 4:61 α + β. *B*, time constants of current relaxation at −50 mV plotted against Ca^{2+} concentration for representative patches for different α-subunit variants alone (α) or α co-expressed with bovine β-subunit (α + β). Dashed lines in *A* signify zero current level.

be restricted to the middle region of the basilar papilla (Fig. 1*B*) and its distribution differed from that of the 4:3, 31:3 and 4:61 variants (Jones *et al.* 1998). The reduced sequence, 4:−26, was functional when expressed in *Xenopus* oocytes and produced Ca^{2+}-activated K^+ channels with unitary conductance (311 pS) comparable to those measured for the other isoforms. Single channels of all alternatively spliced isoforms had linear current–voltage relationships in symmetrical K^+ solutions (Fig. 2). There was no systematic trend among the isoforms in single channel conductance, which had an overall mean (± 1 S.E.M.) of 286 ± 16 pS, in reasonable agreement with the value measured for the native channel in turtle hair cells (Art *et al.* 1995).

Functional properties of α-subunit isoforms

Alternative splicing affected both the apparent Ca^{2+} sensitivity and the kinetics of the heterologously expressed α-subunits (Figs 3 and 4). Voltage activation curves were constructed from tail currents, I, measured at a holding potential of −80 mV in different Ca^{2+} concentrations. They were fitted with a single Boltzmann relationship, B:

$$B = I/I_{max} = 1/(1 + \exp(V_{½} - V)/V_e), \quad (1)$$

where I_{max} is the maximum current, V is the membrane potential, $V_{½}$ is the half-activation voltage, and V_e is the slope factor. Disparities in Ca^{2+} sensitivity between the isoforms were evident in the value of $V_{½}$ at 5 μM Ca^{2+} where there was an 80 mV difference between the channels of greatest (4:61) and least (4:−26) sensitivity. Plots of $V_{½}$ against log[Ca^{2+}] for the different isoforms were displaced relative to one another along the abscissa and there was less evidence of an abrupt slope change in some isoforms than in others (Fig. 4). These two factors accentuated the differences in Ca^{2+} sensitivity between the isoforms at membrane potentials within the physiological range of the hair cell (−70 to −20 mV; Crawford & Fettiplace, 1980). Thus the half-saturating Ca^{2+} concentrations at the hair cell resting potential of −50 mV were 6 μM (4:61), 39 μM (0:0), 200 μM (31:3) and ~250 μM (0:3, 4:3, 4:−26).

There were also kinetic differences among the isoforms that were quantified from the relaxation time constant of the current on repolarization to −50 mV. The current relaxations were fitted with a single exponential decay that in 5 μM Ca^{2+} ranged between 0·9 and 3·6 ms for the different isoforms and was related to their respective Ca^{2+} sensitivities. A slightly better fit was obtained with two exponentials, in which case

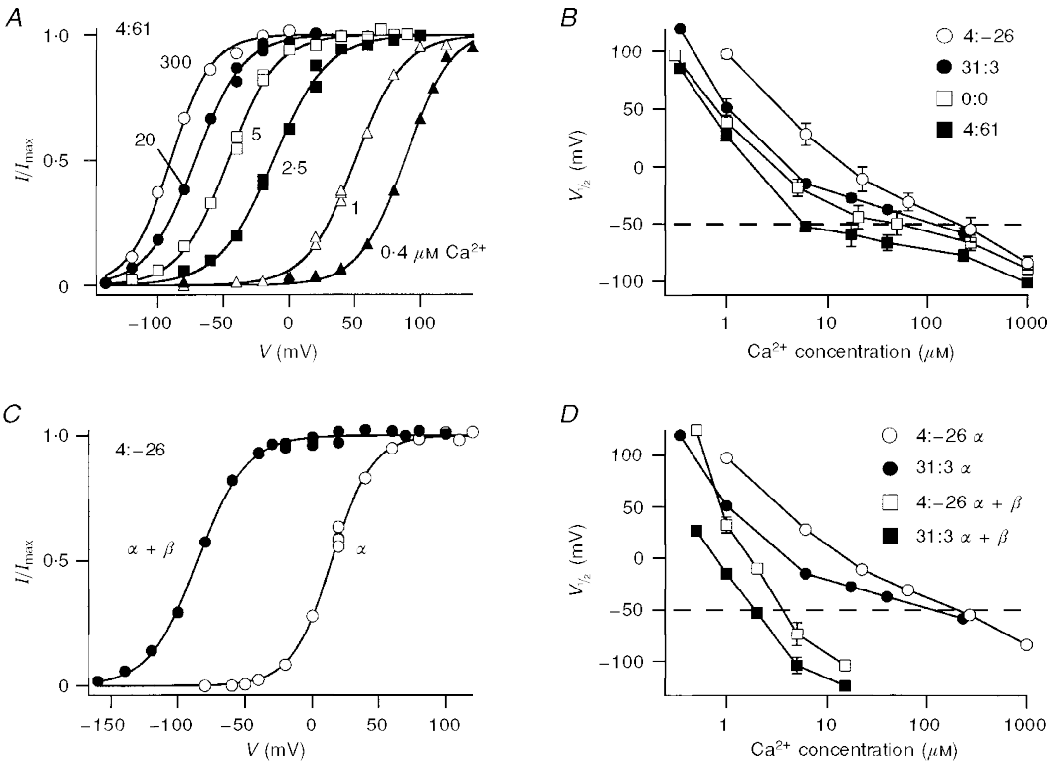

Figure 4. Ca^{2+} sensitivities of different splice variants

A, voltage activation of current (I) of 4:61 α-subunit channels derived from tail current measurements at −80 mV. Each set of points, corresponding to a different Ca^{2+} concentration, was fitted with a Boltzmann relationship: $I/I_{max} = 1/(1 + \exp(V_{½} - V)/V_e)$, where $I_{max} = 3{\cdot}7$ nA. Ca^{2+} concentrations (in μM) for each symbol are indicated. *B*, $V_{½}$ values derived from results similar to those in *A* plotted against Ca^{2+} concentration for different α-subunit isoforms. *C*, voltage activation of 4:−26 α-subunit and 4:−26 α + β-subunit (0·1 β/α mole ratio) channels derived from tail current measurements in 5 μM Ca^{2+}; results were fitted with Boltzmann relationships as in *A*. *D*, effects of β-subunit on the $V_{½}$ *versus* Ca^{2+} concentration plot for the 4:−26 and 31:3 variants.

both components varied with the particular isoform, but for ease of comparison with the hair cell data (Art *et al.* 1995) only the single exponential values are quoted. The relaxation time constants increased with Ca^{2+} concentration (Fig. 3), and as a consequence, at saturating Ca^{2+} levels there was a factor of two difference between the fastest variants (0:3 and 4:3) and the slowest variants (31:3 and 4:61).

Co-expression of α- and β-subunits

Co-expression of any α-subunit isoform with bovine tracheal β-subunit substantially increased the Ca^{2+} sensitivity of the channel. The sensitization was manifested by an approximately 100 mV hyperpolarizing shift in $V_{½}$ in 5 μM Ca^{2+} (Figs 4 and 5). Despite a large disparity in the Ca^{2+} sensitivities of the α-subunits, the negative shift in $V_{½}$ produced by the β-subunit was similar for all variants (Fig. 5). The shift ranged from 89 to 124 mV for the variants 31:3, 4:61, 0:0, 4:−26 and 4:3, with a mean value of 103 mV. The similarity in the $V_{½}$ shift between variants suggests that potentiation by the β-subunit may operate via a mechanism distinct from that produced by exon insertion or deletion at SS1 and SS2. A second consequence of β-subunit co-expression was an approximate 10-fold slowing of the channel kinetics, as previously reported by Dworetzky *et al.* (1996). Thus for the 4:−26 α-subunit, the time constant at −50 mV increased from 0·9 to 10 ms, and for the 4:61 α-subunit, it increased from 3·6 to 46 ms. There was a suggestion that the voltage activation became less steep on addition of the β-subunit. The mean value (± 1 standard deviation) of V_e was 19·3 ± 2·7 mV, averaged over all six α-subunit isoforms, and 22·5 ± 2·5 mV for the $\alpha + \beta$-subunits (values of V_e for individual isoforms are given in the legend to Fig. 5). The slope factors (V_e) for α- and $\alpha + \beta$-subunits were significantly different (Student's t test, $P = 0{\cdot}001$).

A consistent feature of channels formed by co-expression of α- and β-subunits was a growth in Ca^{2+} sensitivity and slowing of the kinetics during the first 3 min of a recording. These changes amounted to a 20–30 mV negative shift in the activation curve and a 2-fold slowing of the current relaxation in a given Ca^{2+} concentration. The changes were unaffected by addition to the intracellular surface of 0·1 μM okadaic acid, to block endogenous protein phosphatases, 3 mM MgATP, or exposure to Ca^{2+}-free (10 mM EGTA) solution. The growth in sensitivity was too slow to stem from a hindered diffusion of Ca^{2+} to the membrane. It implies that the channel properties are modified by intracellular factors that are disrupted on detachment of the membrane patch. Measurements were not taken until the channel sensitivity had stabilized and the negative shifts quoted for co-expression with β-subunit represent steady-state values. The initial sensitization after patch excision was not observed with the α-subunit alone.

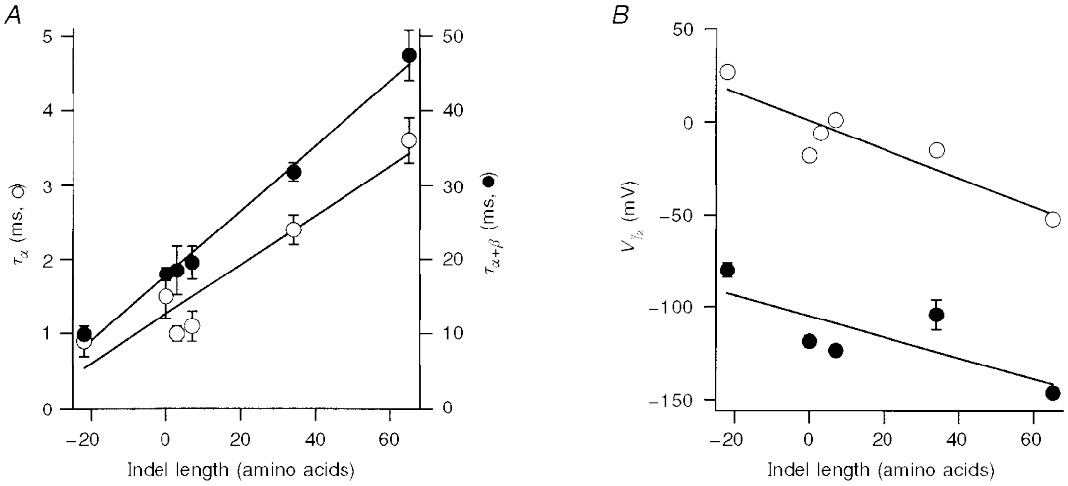

Figure 5. Dependence of K_{Ca} channel properties on size of the amino acid insert or deletion (indel length)

A, time constants of current relaxation at −50 mV plotted *versus* the number of amino acids inserted or deleted at SS1 and SS2 splice sites. ○ (left-hand ordinate): α-subunit alone, 5 μM Ca^{2+}; ● (right-hand ordinate): $\alpha + \beta$-subunits, 2·5 μM Ca^{2+}. Straight lines are least-squares fits with slope (in milliseconds per amino acid; ms AA^{-1}) and regression coefficient: α: 0·033 ms AA^{-1}, 0·953; $\alpha + \beta$: 0·436 ms AA^{-1}, 0·996. *B*, $V_{½}$ *versus* the number of amino acids inserted or deleted at SS1 and SS2 splice sites. ○, α-subunit alone; ●, $\alpha + \beta$-subunits. $V_{½}$ values were obtained by fitting Boltzmann relationships (see Fig. 4) to tail current amplitudes in 5 μM Ca^{2+}. Straight lines are least-squares fits of slope (in millivolts per amino acid; mV AA^{-1}) and regression coefficient: α: −0·77 mV AA^{-1}, 0·905; $\alpha + \beta$: −0·56 mV AA^{-1}, 0·77. All points are means ± 1 S.E.M. The number of measurements averaged for each variant and mean values for Boltzmann slope factor, V_e (in mV), respectively, were: 4:−26 α: 12, 16·6; 0:0 α: 9, 19·8; 0:3: 6, 17·2; 4:3 α: 5, 17·2; 31:3 α: 5, 19·9; 4:61 α: 10, 20·0; 4:−26 $\alpha + \beta$: 9, 22·2; 0:0 $\alpha + \beta$: 3, 24·1; 4:3 $\alpha + \beta$: 3, 24; 31:3 $\alpha + \beta$: 6, 23; 4:61 $\alpha + \beta$: 5, 19.

A convenient means of summarizing the effects of alternative splicing is to plot channel properties as a function of the 'indel length' (Pascarella & Argos, 1992), the combined size of the amino acid insert or deletion at the two splice sites (Fig. 5). The indel length varies from −22 residues for the 4:−26 variant to +65 residues for the 4:61 variant. Figure 5 shows that there were linear relationships between the indel length and both the value of $V_{½}$ and the relaxation time constant at a fixed Ca^{2+} concentration. Larger inserts resulted in slower channels that were activated at more negative voltages. Moreover, the linear relationship held for channels formed from pure α-subunits and those modified by co-expression of β-subunits. The observation that the results for 31:3 and 4:61 variants lay on this relationship suggests that inserts at both splice sites, SS1 and SS2, contribute to the apparent Ca^{2+} sensitivity and kinetics of the channel. Thus the important factor may be the total length of the SS1–SS2 region rather than specific inserts at SS1 or SS2. However, it must be stressed that the different inserts may have more complex effects than are conveyed by Fig. 5, because they can also alter the degree of curvature of the $V_{½}$–log[Ca^{2+}] plot.

Gradation in the effects of the β-subunit

Co-expression with the β-subunit provides a means of regulating the channel kinetics, which raises the possibility that variable amounts of β may produce channels with intermediate properties. To test the feasibility of this mechanism, we co-expressed different proportions of β-subunit and 4:−26 α-subunit by injecting the respective cRNAs in various mole ratios between 0·0003 and 2. The roughly 100 mV shift in $V_{½}$ in 5 μM Ca^{2+} (Fig. 5) reflects a maximal effect of the β-subunit, which was unaffected by reducing the β/α mole ratio from 2 (106 mV, mean shift in $V_{½}$) to 0·1 (103 mV, mean shift in $V_{½}$). However, as the mole ratio was reduced further below 0·01, the shift in $V_{½}$ was diminished, and at the lowest mole ratios, the voltage activation curve approximated that for the α-subunit alone (Fig. 6*A*). In the transition region, for mole ratios between 0·001 and 0·01, the voltage activation curve had a reduced slope, indicative of the mixing of two populations of channels with disparate values of $V_{½}$.

The results were analysed by assuming that the voltage dependence was generated by the sum of two Boltzmann relationships, $B_α$ and $B_{α+β}$, corresponding to α alone and α fully affected by β (Fig. 6*B*). The normalized current for the two extreme mole ratios (0·1 and 0·0003) was each fitted with a single Boltzmann relationship (eqn (1)), where the fit for the 0·0003 mole ratio approximates $B_α$ and that for the 0·1 mole ratio represents $B_{α+β}$. These fits had similar slope factors, $V_ε$, but half-activating voltages, $V_{½}$, which differed by 86 mV. The normalized current for intermediate ratios could then be described by:

$$B_{mix} = f B_α + (1 - f)B_{α+β}, \quad (2)$$

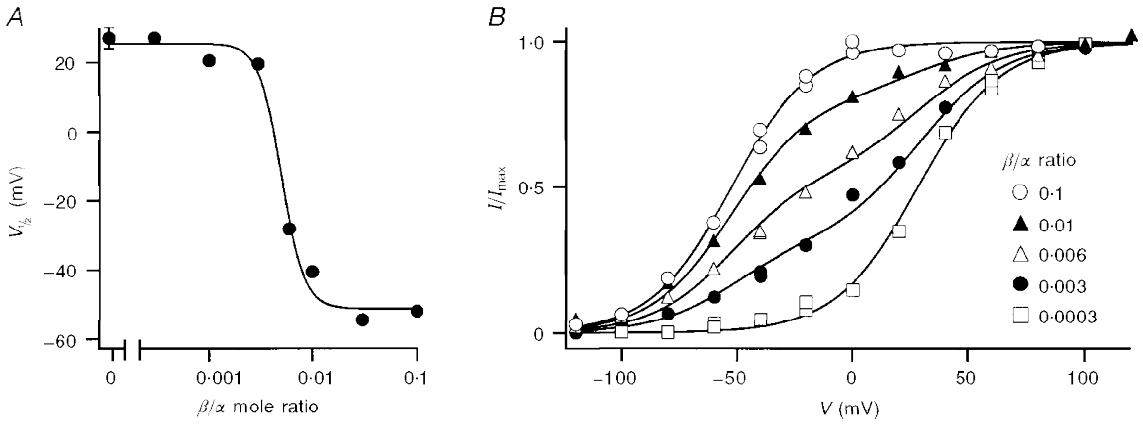

Figure 6. Titration of the shift in voltage sensitivity of the 4:−26 isoform with concentration of β-subunit

A, $V_{½}$ of macroscopic currents in 5 μM Ca^{2+} for patches from oocytes injected with different mole ratios (*R*) of β-subunit to 4:−26 α-subunit cRNA. $V_{½}$ values were obtained by fitting Boltzmann relationships (see Fig. 4) to tail current amplitudes, each point being the mean of two measurements. The mean value (± 1 S.E.M.) for the pure α-subunit alone is included for comparison and a smooth curve has been drawn through the points. Owing to differences in the time course of expression of the β- and α-subunits, all measurements on the titration curve were performed at the same time after mRNA injection in the same batch of oocytes. *B*, examples of voltage–activation relationships in 5 μM Ca^{2+} for the 4:−26 α-isoform in the presence of different amounts of β-subunit. Current, *I*, normalized to its maximum value, I_{max}, was plotted against membrane potential. For the extreme β/α mole ratios each set of points was fitted with a single Boltzmann relationship: $B = I/I_{max} = 1/(1 + \exp(V_{½} - V)/V_ε)$. For $R = 0·0003$, identical to pure α ($B_α$), $V_{½} = 28$ mV, $V_ε = 17·8$ mV. For $R = 0·1$, corresponding to maximal effect of β ($B_{α+β}$), $V_{½} = -58$ mV, $V_ε = 17$ mV. The three intermediate mole ratios were fitted with: $fB_α + (1 - f)B_{α+β}$, where $f = 0·19$ ($R = 0·01$), 0·45 ($R = 0·006$) and 0·69 ($R = 0·003$). The results indicate the presence of only two species of channel, composed of α alone or α fully affected by β.

where f, the fraction of channels composed of α alone, decreased from 0·69 to 0·19 as the mole ratio increased from 0·003 to 0·01 (Fig. 6*B*). The quality of the fits supports the assumption that the macroscopic current results from the mixing of only two channel species, α alone and α fully affected by β; moreover, the results imply that the β-subunit has an all-or-none affect on the Ca^{2+} sensitivity of the channel. Similar results (not shown) were also obtained by titrating the effects of β-subunit concentration on the 31:3 α isoform.

Effects of β-subunit on single-channel properties

The mixing of the β- and 4:—26 α-subunits was further investigated by examining the kinetic properties of single K_{Ca} channels (Fig. 7). Expression of a maximal β-subunit concentration produced a 5-fold increase in the mean open time (τ_o) of the channels compared with that obtained with a pure α-subunit alone. Measurements on 24 single channels from oocytes injected with low β/α ratios of 0·003 to 0·01 showed that the values of τ_o fell into two distinct categories with means of 1·1 and 4·7 ms, which were identified as pure α and an $\alpha + \beta$-component. The identification of pure α is consistent with the open time distribution for channels in oocytes injected with 4:—26 α only, depicted as the hatched population in Fig. 7*C*. There was no evidence that the $\alpha + \beta$-component, though relatively broad, contained multiple peaks at intermediate open times. For a 1/1 β/α stoichiometry, such intermediate peaks might have been expected, corresponding to one, two, three or four β-subunits per channel, assuming a tetrameric channel (Shen *et al.* 1994). The β-subunit must also exert an all-or-none effect on channel kinetics.

The increase in mean open time produced by the β-subunit is qualitatively consistent with the slowing of the kinetics of the macroscopic current, but the open times for the $\alpha + \beta$-mixtures were briefer than the relaxation time constants of the macroscopic currents. An explanation for this discrepancy

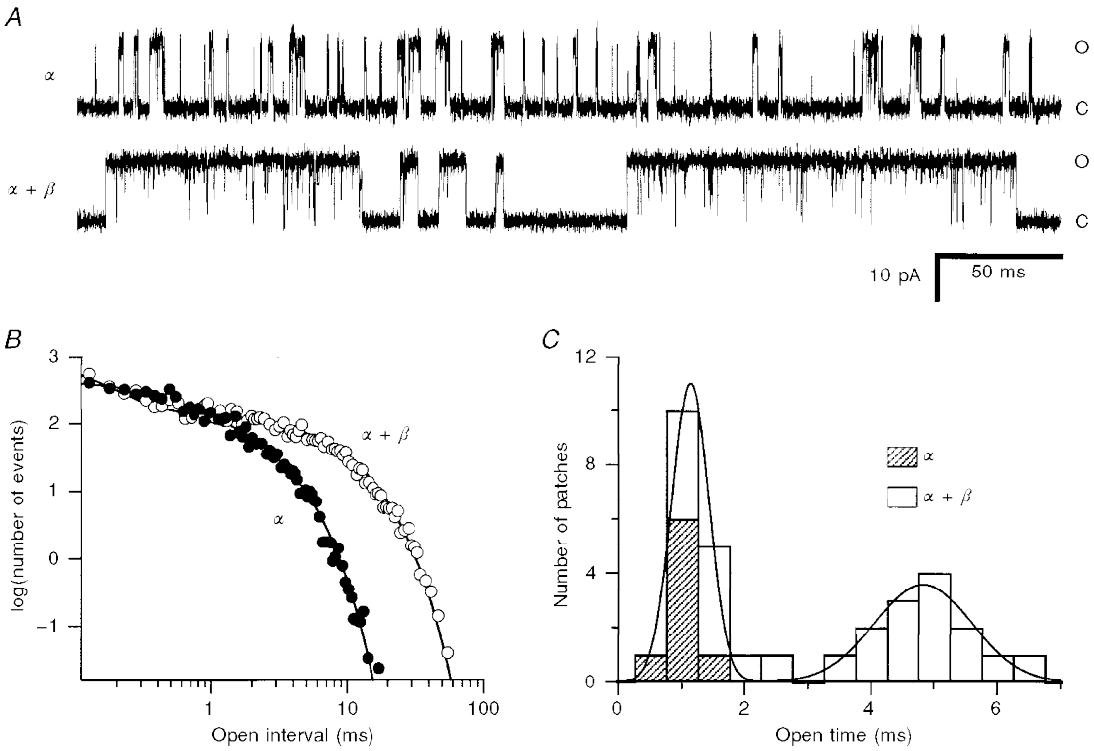

Figure 7. Effects of co-expression of β-subunit on 4:—26 α-subunit channels

A, single-channel records at −50 mV for pure α- and $\alpha + \beta$-subunits. Ca^{2+} concentrations, chosen to give similar probabilities of opening (~0·2) in the two recordings, were: α, 15 μM; $\alpha + \beta$, 2·5 μM. Note that channel events with β-subunit consist of long bursts of openings interrupted by very brief closures. Closed and open levels are indicated by C and O, respectively. *B*, open time distributions of α- and $\alpha + \beta$-subunit channels shown in *A*, the ordinate scale denoting the number of events per 25 μs bin derived from recordings 50 s in duration. To compensate for differences in numbers of events in the two recordings, the data for the $\alpha + \beta$-channel were multiplied by 6·1 to superimpose the distributions at short intervals. Smooth lines are maximum likelihood fits to sums of two components with time constants of 0·40 and 1·6 ms (α) and 0·13 and 5·8 ms ($\alpha + \beta$). *C*, mean open times of channels derived from oocytes injected with α-subunit alone (▨) and oocytes injected with $\alpha + \beta$-subunits at β/α mole ratios of 0·003–0·1. Only the slow component of the open time is plotted. The smooth curve is the fit with the sum of two Gaussians with mean ± 1 standard deviation of 1·1 ± 0·4 and 4·8 ± 1·1 ms, respectively.

is that the channel openings occur in bursts, and the mean burst length determines the macroscopic kinetics. A burst analysis was applied to the single-channel records (see Methods) and gave a mean burst length for 4:−26 $\alpha + \beta$-channels of 25 ± 2 ms ($n = 12$ observations). This value was different from the mean open time in this population, which was 5·1 ± 0·2 ms. The burst duration was most consistent with the relaxation time constant (τ_R) determined for the ensemble average of single-channel currents in response to voltage steps from +50 to −50 mV (the same protocol employed to categorize the macroscopic current kinetics). Two 4:−26 $\alpha + \beta$-channels had a mean open time of 5·4 ms compared with a mean τ_R of 25 ms, a value similar to the mean burst length. In contrast, for the 4:−26 α-subunit alone, the mean burst length (1·5 ± 0·2 ms, $n = 8$) was scarcely different from the mean open time (1·3 ± 0·1 ms, $n = 8$). These observations may be explained by supposing that the β-subunit stabilizes the open state of the channel.

Effects of co-expression with avian β2-subunits

Another protein, CO6, resembling the K_{Ca} channel β-subunit, has recently been cloned from avian (quail and chicken) fibroblasts (Oberst *et al.* 1997) and shown to occur in the chick cochlea and to produce β-like effects in expression studies (Ramanathan *et al.* 1999). This protein has significant structural homology with the mammalian β-subunit, based on hydropathy plots, but only 47% amino acid identity (Oberst *et al.* 1997). It is thus likely to be encoded by a different gene, and will be denoted as a β2-subunit. Co-expression of the β2-subunit from either quail (ccβ2) or chicken (ggβ2) had effects on the K_{Ca} channel properties that were qualitatively similar to those of the bovine β-subunit (Fig. 8). In all α-isoforms studied, the

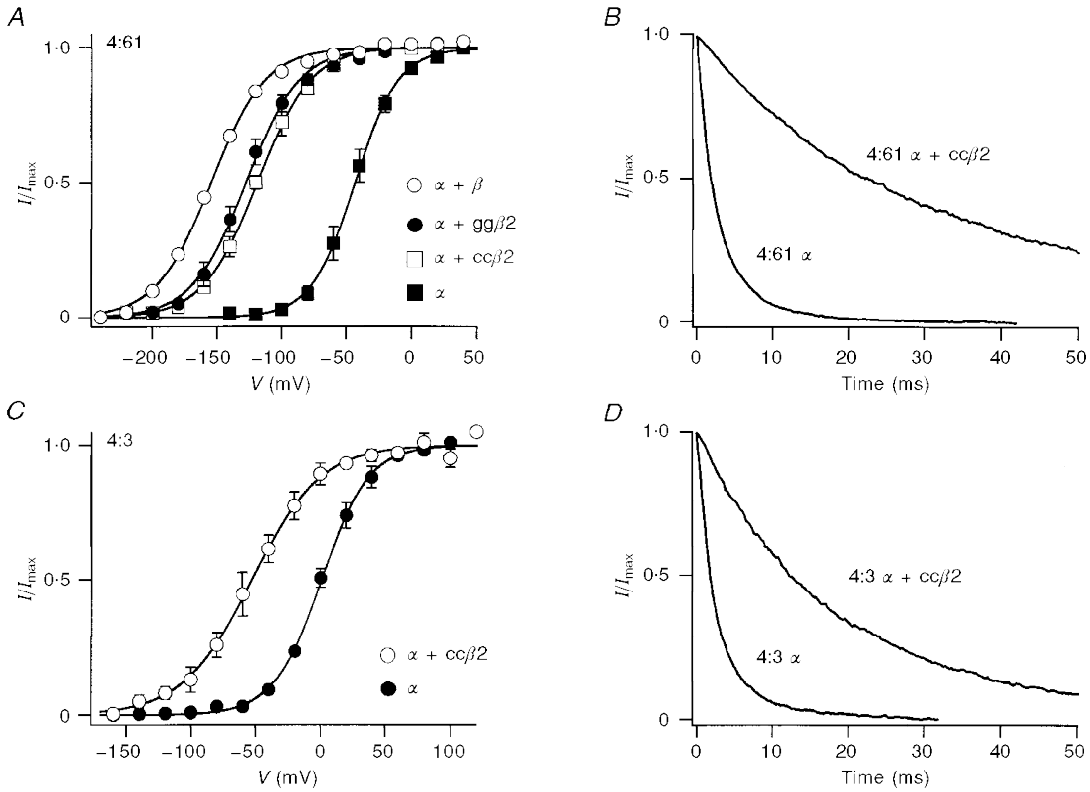

Figure 8. Effects of avian β2-subunit on the properties of 4:61 and 4:3 α-subunit isoforms

A, voltage activation in 5 μM Ca^{2+} for a 4:61 α-subunit co-expressed with different β-subunits. Each set of points is the mean current (I), normalized to its maximum value (I_{max}), and has been fitted with a Boltzmann function (eqn (1)). Fitting parameters for $V_{½}$ and slope factor V_e, and the number of experiments averaged for each condition were: α: −44 mV, 17 mV, 3; α + bovine β: −155 mV, 21 mV, 1; α + ccβ2 (quail): −119 mV, 21 mV, 3; α + ggβ2 (chicken): −128 mV, 21 mV, 3. *B*, normalized tail currents measured at −80 mV holding potential for 4:61 α-subunit alone, or α-subunit co-expressed with quail β2 (α + ccβ2). Time constants of decay of the tail current were 3·2 ms (α) and 37 ms (α + ccβ2). *C*, voltage activation in 5 μM Ca^{2+} for 4:3 α alone and when co-expressed with quail β-subunit (α + ccβ2). Boltzmann fitting parameters for $V_{½}$ and V_e, and the number of experiments averaged for each condition were: α: 1 mV, 18 mV, 4; α + ccβ2 (quail): −53 mV, 27 mV, 4. *D*, normalized tail currents measured at −50 mV holding potential for 4:3 α-subunit alone, or α-subunit co-expressed with quail β2 (α + ccβ2). Time constants of decay of the tail currents were 3·1 ms (α) and 21 ms (α + ccβ2). In both *A* and *C*, bars are ± 1 S.E.M.

avian $\beta 2$ produced a slowing of channel kinetics and a hyperpolarizing shift in the activation curve, though the extent of the shift was less than that with bovine β. The activation curve for 4:61 α was shifted 80 mV negative with avian $\beta 2$ compared with 112 mV with bovine β in the same batch of oocytes (Fig. 8*A*). The avian cc$\beta 2$ caused a mean negative shift of 54 mV with 4:3 α (Fig. 8*C*), 50 mV with 31:3 α and 40 mV with 4:−26 α. These values were about half the shift of approximately 100 mV measured with bovine β in separate experiments (Fig. 5*B*), and they suggest that $\beta 2$, like β, preserves relative differences in Ca^{2+} sensitivity between α-isoforms.

31:3 and 4:−26 were two of the least Ca^{2+}-sensitive isoforms, requiring over 200 μM Ca^{2+} for half-activation at −50 mV (Fig. 4*B*). Co-expression of cc$\beta 2$ reduced the half-activating Ca^{2+} concentration at −50 mV to $5{\cdot}7 \pm 0{\cdot}8$ μM ($n = 3$) for 31:3, and to 12·6 μM ($n = 2$) for 4:−26. For both α-isoforms, co-expression of cc$\beta 2$ also slowed the relaxation time constant at −50 mV by approximately 10-fold. Thus for 31:3, the time constant increased from $2{\cdot}4 \pm 0{\cdot}3$ ms ($n = 6$) with the α-subunit alone to 25 ± 5 ms ($n = 5$) when co-expressed with cc$\beta 2$; for 4:−26, co-expression with cc$\beta 2$ increased the time constant from $1{\cdot}2 \pm 0{\cdot}1$ ms ($n = 6$) to 13 ± 2 ms ($n = 5$). These results demonstrate that the avian $\beta 2$, though dissimilar in sequence, exhibits effects comparable to those of bovine β.

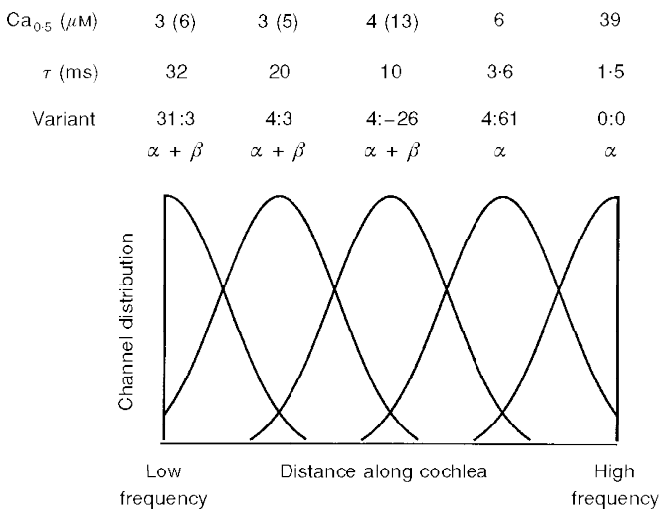

Figure 9. Hypothetical distribution of K_{Ca} channel subunits to account for the tonotopic organization of the turtle cochlea

The hair cell concentration of each isoform is plotted against distance along the cochlea from the low-frequency end. Only the 31:3 $\alpha + \beta$, 4:3 $\alpha + \beta$, 4:−26 $\alpha + \beta$, 4:61 α, and 0:0 α variants are shown, calculated as overlapping Gaussian distributions in decreasing order of time constant. Experimental values for the relaxation time constant (τ) and half-saturating $[Ca^{2+}]$ ($Ca_{0.5}$) at −50 mV for the different variants are shown above the plot. The $Ca_{0.5}$ values given in parentheses were obtained for the avian $\beta 2$; all other values are for bovine β. Evidence in support of the scheme is described in the text.

DISCUSSION

Mechanisms of the differences between the variants

The considerable sequence variability generated by alternative splicing at SS1 and SS2 implies that this region is functionally important in controlling the channel properties. This notion is confirmed by the large differences in the apparent Ca^{2+} sensitivity between splice variants, which can be increased by large inserts and reduced by deletions around SS1 and SS2. Whether the region constitutes part of the Ca^{2+}-binding site is unclear since at least one portion of the Ca^{2+} sensor is thought to lie a significant distance downstream of SS2, just proximal to the tenth amphipathic α-helix (Fig. 1; Schreiber & Salkoff, 1997). The complexity of splicing resembles that observed in *dSlo* at site G (Lagrutta *et al.* 1994), which is equivalent to the region spanning SS2 in vertebrate *Slo*. However, the *Drosophila* splice variants differed mainly in their kinetics but not Ca^{2+} sensitivity.

By what mechanism might the splice variants influence channel gating? Differences among variants in the $V_{½}$–log$[Ca^{2+}]$ relationships could in theory be caused by alterations in the Ca^{2+}-binding site, gating charge or degree of co-operativity between subunits (see Fig. 15 of Cox *et al.* 1997). However, the convergence of the experimental plots at high Ca^{2+} concentration suggests that neither subunit co-operativity nor Ca^{2+} affinity alone can explain the differences between splice variants. The effects of alternative splicing on the $V_{½}$–log$[Ca^{2+}]$ relationships resemble the effects of mutations in the S4–S5 intracellular loop (Sullivan *et al.* 1997), which shift the relationship to higher Ca^{2+} concentrations and reduce its slope. To account for the importance of the alternatively spliced segment, it may be speculated that Ca^{2+} binding facilitates an interaction of the intracellular domain encompassing the two splice sites, SS1 and SS2, with the S4–S5 loop. Such an interaction could then influence the voltage-sensing S4 domain to culminate in channel opening. The free energy of the interaction may depend on the size of the SS1–SS2 segment which, due to alternative splicing, varies in length from 40 amino acids in the 4:−26 isoform to 127 amino acids in the 4:61 isoform. One possibility is that steric factors related to the length of the segment affect the energy barrier, shorter segments being less likely to result in channel opening. This mechanism would be consistent with the results shown in Fig. 5, which demonstrate a linear relationship between the indel length and the channel kinetics or $V_{½}$ for voltage activation in fixed $[Ca^{2+}]$.

Role of variants in generating diversity of frequency tuning

Most of the α-subunit isoforms apart from 4:61 and 0:0 were less Ca^{2+} sensitive than the native K_{Ca} channel of the hair cell, within the physiological range of membrane potentials. For example, the Ca^{2+} concentrations required for half-activation at −50 mV were 6 μM (4:61) and 39 μM (0:0), but 200 μM or more for the other isoforms (Fig. 4).

These values may be compared with 12 μM (range, 5–30 μM) for the native channel of the hair cell (Art *et al.* 1995), which suggests that most of the splice variants are likely to be complexed with an auxiliary subunit. We have no evidence for a K_{Ca} channel β-subunit in the turtle cochlea, but there is a report that a protein, CO6, homologous to the β-subunit (Oberst *et al.* 1997), is present in the chicken cochlea (Ramanathan *et al.* 1999). CO6 has been labelled as a β2-subunit which, it should be noted, is distinct from a third auxiliary subunit that confers inactivation on K_{Ca} channels (Wallner *et al.* 1999). Our results (Fig. 8) indicate that the effects of the avian β2-subunit are qualitatively similar to those of the bovine β-subunit. The β2-subunit slowed the current relaxations by an amount (10-fold) virtually identical to that produced by the bovine β-subunit; also, it enhanced the Ca^{2+} sensitivity of all isoforms, though by a smaller extent than that caused by the bovine β-subunit. Our β2 results largely agree with the expression data of Ramanathan *et al.* (1999). However, their observation that β2 equalized the Ca^{2+} affinities of two alternatively spliced α-isoforms (0:0 and 0:61) was not reflected in our results, where relative differences in Ca^{2+} sensitivity between α-isoforms were retained on co-expression with the β2 subunit.

If only those combinations with high Ca^{2+} sensitivity are considered, then their kinetics at −50 mV in 5 μM Ca^{2+} range from 1·5 ms (0:0 α-subunit) to 45 ms (4:61 α + β-subunit). While the overall (30-fold) kinetic range is comparable for the native and cloned channels, the absolute time constants are severalfold faster for the native channels (range, 0·4–14 ms in 4 μM Ca^{2+}; Art *et al.* 1995). It is notable that channels with high Ca^{2+} sensitivity and very fast kinetics (∼0·5 ms), characteristic of hair cells tuned to high frequencies, had no equivalent in the expressed channels. Such fast channels may be the product of still unidentified α- or β-subunits. It is also possible that the performance of the channel in the hair cell differs quantitatively from its behaviour in the oocytes. Such differences may depend on the local cellular environment, including membrane lipid composition (Bolotina *et al.* 1989) and attachments to other auxiliary proteins (e.g. Slob; Schopperle *et al.* 1998). One manifestation of such cytoplasmic effects may be the 2-fold slowing in kinetics observed on excision of the oocyte patch (see Results).

The tonotopic map

Owing to the tonotopic arrangement of the turtle cochlea (Crawford & Fettiplace, 1980), the K_{Ca} channel kinetics must change systematically along the hair cell epithelium. Since the β-subunit exerts an all-or-none effect on the properties of a given α-subunit isoform (Figs 6 and 7), a cochlear β-subunit concentration gradient cannot account for the tonotopic organization. However, a β-subunit gradient combined with differential expression of α-subunit isoforms (Jones *et al.* 1998) may underlie the frequency map in the turtle cochlea. Thus it is envisaged that the least Ca^{2+}-sensitive isoforms (4:3, 4:−26 and 31:3) would be complexed with β-subunit to produce slow K_{Ca} channels in low-frequency hair cells, whereas the most Ca^{2+}-sensitive isoforms (4:61 and 0:0) would, in the absence of a β-subunit, form fast channels in cells tuned to high frequencies.

Figure 9 shows a possible cochlear distribution of K_{Ca} channel variants, where the time constant of current relaxation at −50 mV ranges from 32 ms at the low-frequency end to 1·5 ms at the high-frequency end of the cochlea. Although the exact (Gaussian) distribution for each variant is arbitrary, their placement is largely consistent with present evidence (Fig. 1*B*; Jones *et al.* 1998). The 31:3 and 4:3 variants were detected only at the low-frequency end, 4:−26 was present in the mid-papillar region and 4:61 occurred predominantly at the high-frequency end. The 0:0 variant, though not solely restricted to the high-frequency end, was the only variant detected there other than 4:61. A central assumption in Fig. 9, that the β-subunit is expressed only in the low-frequency half, is supported by the results of Ramanathan *et al.* (1999) who found a concentration gradient in β2-subunit message from the apical to basal end of the chicken cochlea. An implication is that the β-subunit is not present in those hair cells containing the 4:61 α-subunit. A similar arrangement may exist in rat adrenal chromaffin cells that express K_{Ca} α-subunits with SS2 58 or 61 inserts, homologous to the SS2 61 insert in turtle hair cells. It has been argued that no β-subunit is needed to account for the native K_{Ca} channels in chromaffin cells because the Ca^{2+} sensitivity of the α-subunits with 58 or 61 amino acid inserts closely matches that of K_{Ca} channels recorded in the intact cell (Xie & McCobb, 1998). We conclude that differential expression of a few alternatively spliced α-subunit variants, coupled with a non-uniform cochlear distribution of a β-subunit, can produce a range of K_{Ca} channel properties required to explain the frequency range and tonotopic organization of the turtle cochlea.

The small number of variants depicted in Fig. 9 implies that there might be discontinuities in resonant frequency as the hair cells shift from use of one isoform to another. However, several factors could conspire to smooth out the frequency map. Firstly, there are other isoforms (e.g. 31:0 and 4:0; see also Jones *et al.* 1998) not yet characterized that could possess distinct properties. Secondly, each cell may express several variants in unique proportions (Navaratnam *et al.* 1997), each producing a homomultimer, in which case the kinetics of the macroscopic K_{Ca} current would be an average for the specific channel mixture. Mixing of a total of five channel types similar to those in Fig. 9 was shown theoretically to be capable of generating a continuous frequency map (Wu & Fettiplace, 1996). Finally, two α-isoforms may form heteromultimers that give rise to channels of intermediate properties. We have preliminary results that at least two of the splice variants (0:0 and 4:−26) when co-expressed produce channels with kinetics and Ca^{2+} sensitivity midway between those of the homomeric channels of the individual isoforms.

Art, J. J. & Fettiplace, R. (1987). Variation of membrane properties in hair cells isolated from the turtle cochlea. *Journal of Physiology* **385**, 207–242.

Art, J. J., Wu, Y.-C. & Fettiplace, R. (1995). The calcium-activated potassium channels of turtle hair cells. *Journal of General Physiology* **105**, 49–72.

Bers, D. M., Patton, C. W. & Nuccitelli, R. (1994). A practical guide to the preparation of calcium buffers. *Methods in Cell Biology* **40**, 3–29.

Bolotina, V., Omelynenko, V., Heyes, B., Ryan, U. & Bregestowksi, P. (1989). Variations of membrane cholesterol alter the kinetics of Ca^{2+}-dependent Ca^{2+} channels and membrane fluidity in vascular smooth muscle. *Pflügers Archiv* **415**, 262–268.

Butler, A., Tsunoda, S., McCobb, D. P., Wei, A. & Salkoff, L. (1993). *mSlo*, a complex mouse gene encoding 'maxi' calcium-activated potassium channels. *Science* **261**, 221–224.

Colquhoun, D. & Sackmann, B. (1985). Fast events in single-channel currents activated by acetylcholine and its analogues at the frog neuromuscular end-plate. *Journal of Physiology* **369**, 501–557.

Cox, D. H., Cui, J. & Aldrich, R. W. (1997). Allosteric gating of a large conductance Ca-activated K^+ channel. *Journal of General Physiology* **110**, 257–281.

Crawford, A. C. & Fettiplace, R. (1980). The frequency selectivity of auditory nerve fibres and hair cells in the cochlea of the turtle. *Journal of Physiology* **306**, 79–125.

Dichiara, T. J. & Reinhart, P. H. (1997). Redox modulation of *hslo* Ca^{2+}-activated K^+ channels. *Journal of Neuroscience* **17**, 4942–4955.

Dworetzky, S. I., Boissard, C. G., Lum-Regan, J. T., McKay, M. C., Post-Munson, D. J., Trojnacki, J. T., Chang, C.-P. & Gribkoff, V. K. (1996). Phenotypic alteration of a human BK (*hSlo*) channel by *hSlo*β subunit coexpression: changes in blocker sensitivity, activation/relaxation and inactivation kinetics, and protein kinase A modulation. *Journal of Neuroscience* **16**, 4543–4550.

Jiang, G.-J., Zidanic, M., Michaels, R. L., Michael, T. H., Griguer, C. & Fuchs, P. A. (1997). *cSlo* encodes calcium-activated potassium channels in the chick's cochlea. *Proceedings of the Royal Society* B **264**, 731–737.

Jones, E. M. C., Laus, C. & Fettiplace, R. (1998). Identification of Ca^{2+}-activated K^+ channel splice variants and their distribution in the turtle cochlea. *Proceedings of the Royal Society* B **265**, 685–692.

Kaczorowski, G. J., Knaus, H.-G., Leonard, R. J., McManus, O. B. & Garcia, M. L. (1996). High-conductance calcium-activated potassium channels: structure pharmacology and function. *Journal of Bioenergetics and Biomemembranes* **28**, 255–267.

Lagrutta, A., Shen, K.-Z., North, R. A. & Adelman, J. P. (1994). Functional differences among alternatively spliced variants of *slowpoke*, a *Drosophila* calcium-activated potassium channel. *Journal of Biological Chemistry* **269**, 20347–20351.

McManus, O. B., Helms, L. M., Pallanck, L., Ganetzky, B., Swanson, R. & Leonard, R. J. (1995). Functional role of the β-subunit of high conductance calcium-activated potassium channels. *Neuron* **14**, 645–650.

Meera, P., Wallner, M., Song, M. & Toro, L. (1997). Large conductance voltage- and calcium-dependent K^+ channel, a distinct member of voltage-dependent ion channels with seven N-terminal transmembrane segments (S0–S6), an extracellular N-terminus, and an intracellular (S9–S10) C-terminus. *Proceedings of the National Academy of Sciences of the USA* **94**, 14066–14071.

Navaratnam, D. S., Bell, T. J., Tiu, T. D., Cohen, E. L. & Oberholtzer, J. C. (1997). Differential distribution of Ca^{2+}-activated K^+ channel splice variants among hair cells along the tonotopic axis of the chick cochlea. *Neuron* **19**, 1077–1085.

Oberst, C., Weiskirchen, R., Hartl, M. & Bister, K. (1997). Suppression in transformed avian fibroblasts of a gene (CO6) encoding a membrane protein related to mammalian potassium channel regulatory subunits. *Oncogene* **14**, 1109–1116.

Pascarella, S. & Argos, P. (1992). Analysis of insertions/deletions in protein structures. *Journal of Molecular Biology* **224**, 461–471.

Ramanathan, K., Michael, T. H., Jiang, G.-J., Hiel, H. & Fuchs, P. A. (1999). A molecular mechanism for electrical tuning of cochlear hair cells. *Science* **283**, 215–217.

Robertson, G. A., Warmke, J. M. & Ganetzky, B. (1996). Potassium currents expressed from *Drosophila* and mouse eag cDNAs in *Xenopus* oocytes. *Neuropharmacology* **35**, 841–850.

Robitaille, R. & Charlton, M. P. (1992). Presynaptic calcium signals and transmitter release are modulated by calcium-activated potassium channels. *Journal of Neuroscience* **12**, 297–305.

Rosenblatt, K. P., Sun, Z.-P., Heller, S. & Hudspeth, A. J. (1997). Distribution of Ca^{2+}-activated K^+ channel isoforms along the tonotopic gradient of the chicken's cochlea. *Neuron* **19**, 1061–1075.

Schopperle, W. M., Holmqvist, M. H., Zhou, Y., Wang, J., Wang, Z., Griffith, L. C., Keselman, I., Kusinitz, F., Dagan, D. & Levitan, I. B. (1998). Slob, a novel protein that interacts with the slowpoke calcium-dependent potassium channel. *Neuron* **20**, 565–573.

Schreiber, M. & Salkoff, L. (1997). A novel calcium sensing domain in the BK channel. *Biophysical Journal* **73**, 1355–1363.

Shen, K.-Z., Lagrutta, A., Davies, N. W., Standen, N. B., Adelman, J. P. & North, R. A. (1994). Tetraethylammonium block of Slowpoke calcium-activated potassium channels expressed in *Xenopus* ooccytes: evidence for tetrameric channel formation. *Pflügers Archiv* **426**, 440–445.

Silberberg, S. D., Lagrutta, A., Adelman, J. P. & Magleby, K. L. (1996). Wanderlust kinetics and variable Ca^{2+}-sensitivity of *Drosophila*, a large conductance Ca^{2+}-activated K^+ channel, expressed in oocytes. *Biophysical Journal* **70**, 2640–2651.

Stühmer, W. & Parekh, A. B. (1995). Electrophysiological recordings from *Xenopus* oocytes. In *Single-Channel Recording*, 2nd edn, ed. Sakmann, B. & Neher, E., pp. 341–356. Plenum Press, New York and London.

Sullivan, D. A., Holmqvist, M. H. & Levitan, I. B. (1997). Characterization of gating and peptide block of *mSlo*, a cloned calcium-activated potassium channel. *Journal of Neurophysiology* **78**, 2937–2950.

Tseng-Crank, J., Foster, C. D., Krause, J. D., Mertz, R., Godinot, N., Dichiara, T. J. & Reinhart, P. H. (1994). Cloning, expression, and distribution of functionally distinct Ca^{2+}-activated K^+ channel isoforms from human brain. *Neuron* **13**, 1315–1330.

Tsien, R. W. & Rink, T. J. (1980). Neutral carrier ion-selective microelectrodes for measurement of intracellular free calcium. *Biochimica et Biophysica Acta* **599**, 623–638.

Wallner, M., Meera, P. & Toro, L. (1996). Determinant for β-subunit regulation in maxi K_{Ca} channels. An additional transmembrane region at the N-terminus. *Proceedings of the National Academy of Sciences of the USA* **93**, 14922–14927.

Wallner, M., Meera, P. & Toro, L. (1999). Molecular basis of fast inactivation in voltage and Ca^{2+}-activated K^+ channels: a transmembrane β-subunit homolog. *Proceedings of the National Academy of Sciences of the USA* **96**, 4137–4142.

Wei, A., Solaro, C., Lingle, C. & Salkoff, L. (1994). Calcium-sensitivity of BK-type K_{Ca} channels determined by a separable domain. *Neuron* **13**, 671–681.

Wu, Y.-C., Art, J. J., Goodman, M. B. & Fettiplace, R. (1995). A kinetic description of the calcium-activated potassium channel and its application to electrical tuning of hair cells. *Progress in Biophysics and Molecular Biology* **63**, 131–158.

Wu, Y.-C. & Fettiplace, R. (1996). A developmental model for generating frequency maps in the reptilian and avian cochleas. *Biophysical Journal* **70**, 2557–2570.

Xie, J. & McCobb, D. P. (1998). Control of alternative splicing of potassium channels by stress hormones. *Science* **280**, 443–446.

Acknowledgements

This research was supported by grants to R.F. from NIDCD (DC01362) and the Steenbock Fund of the University of Wisconsin. We thank M. Moscu for technical assistance, Y.-C. Wu for single-channel analysis programs and Miriam Goodman for helpful comments on the manuscript. R. Swanson kindly provided us with the bovine K_{Ca} channel β-subunit and C. Oberst and K. Bister supplied the avian β2-subunits.

Corresponding author

R. Fettiplace: 185 Medical Sciences Building, 1300 University Avenue, Madison, WI 53706, USA.

Email: fettiplace@physiology.wisc.edu

E. M. C. Jones and M. Gray-Keller contributed equally to this work.